Kinetics and Catalysis, Vol. 42, No. 4, 2001, pp. 561–573. Translated from Kinetika i Kataliz, Vol. 42, No. 4, 2001, pp. 618–631.

Formation of the Ni–CrO_x/MgO and Ni/MgO Catalysts for Carbon Dioxide Reforming of Methane

V. Yu. Bychkov, V. N. Korchak, O. V. Krylov, O. S. Morozova, and T. I. Khomenko

Semenov Institute of Chemical Physics, Russian Academy of Sciences, Moscow, 117977 Russia

Received February 24, 2000

Abstract—Temperature-programmed reduction by hydrogen, temperature-programmed desorption of O_2, local X-ray spectral analysis, and scanning electron microscopy are used to study redox processes occurring on the Ni–Cr_2O_3/MgO and Ni/MgO catalysts for carbon dioxide reforming of methane. The reduction of Ni/MgO leads to the formation of nickel clusters distributed over the surface of MgO. During the reduction of NiO–Cr_2O_3/MgO, chromates are transformed into chromites, and then nickel is formed by the reduction of spinel $NiCr_2O_4$. Reoxidation leads to the oxidized structures NiO, $NiCr_2O_4$, and $NiCrO_4$.

INTRODUCTION

Many papers have been published that are devoted to carbon dioxide reforming of methane. Their number is still growing. However, in many cases, researchers are interested in autothermal reforming $CH_4 + CO_2 + O_2$ rather than in the CO_2 and CH_4 reaction itself. The former reaction leads to syngas with a CO : H_2 ratio close to 1 : 1 without substantial heat evolution or consumption. The main difficulty in the simultaneous occurrence of reactions between CO_2 and CH_4 and between CH_4 and O_2 is that one reaction requires a 100–200°C higher temperature than the other (on the same catalyst). Therefore, it is necessary to increase the catalyst activity toward carbon dioxide reforming of methane as much as possible:

$$CH_4 + CO_2 = 2CO + 2H_2. \quad (I)$$

Resistance to coking is less important, because the presence of O_2 reduces coke formation.

In a search for the catalyst with the maximal activity toward reaction (I), we studied a number of nickel catalysts supported on MgO and containing transition metal oxides (Cr_2O_3, CeO_2, MnO_2, and CuO) [1]. The Ni/MgO catalyst modified by Cr_2O_3, the Ni/MgO catalyst containing large amounts of Ni, and the NiO + MgO system prepared by the method of mechanochemical activation were the most active. The additives of CeO_2 and CuO to the Ni–Cr–O_x/MgO and Ni/MgO catalysts did not lead to an increase in the activity. The MnO_2 additive even led to a decrease in the activity.

The oxidation of carbon on the catalyst surface after the reaction was accompanied by the reoxidation of Ni to NiO in Ni/MgO and the transformation of Ni and Cr_2O_3 into $NiCrO_4$ in Ni–Cr–O_x/MgO. In many papers devoted to the mechanism of reaction (I) (see review papers [2–4]), carbon is believed to be an intermediate species, which participates in different process, including redox ones. We may assume that the main reaction itself also occurs via a redox mechanism in which one reagent (CH_4) is a reducing agent, and the other (CO_2) is an oxidant. This mechanism was assumed in different studies, specifically when transition metal oxides were applied as catalysts.

In [5, 6], reaction (I) was studied on the Ni/La_2O_3 catalyst. Lanthanum oxide possesses both basic and redox properties, therefore it was suggested that the rate-limiting step of the process is the reductive decomposition of basic lanthanum carbonate formed in the reaction with CO_2

$$Ni + La_2O_2CO_3 \longrightarrow NiO + CO + La_2O_3. \quad (II)$$

A high catalytic activity was observed in the case of perovskites $La_{1-x}Sr_xNiO_3$ [7] and $Ca_{0.8}Sr_{0.2}NiO_3$ [8], which have both redox and basic properties. In our work [9] devoted to the study of metal-free Mn–Cr oxide catalysts, the reductive decomposition of carbonate in the rate-limiting step was assumed as well:

$$MnCO_3 + Cr_2O_3 + C \longrightarrow MnCr_2O_4 + 2CO. \quad (III)$$

The redox mechanism involving reduction NiO ⟶ Ni and reoxidation Ni ⟶ NiO was also proposed for carbon dioxide reforming of methane over NiO–MgO [10].

This paper reports the results of studies of the possible redox transformations of active catalyst for carbon dioxide reforming of methane on Ni/MgO and Ni–Cr–O_x/MgO (and some others) under the conditions of their formation. The interaction with the reducing agent (H_2) and the oxidant (O_2) can be considered as a model of complex reactions of the catalyst with CH_4 and CO_2. The following methods were chosen for the study: temperature-programmed reduction (TPR) by hydrogen, temperature-programmed desorption (TPD) of O_2, local X-ray spectral analysis (LXSA), and scanning electron microscopy (SEM). We also present data obtained in the TPR study of Ni/MgO catalysts

0023-1584/01/4204-0561$25.00

modified by CuO, CeO_2, and MnO_2, which were studied earlier in [1].

EXPERIMENTAL

Catalysts prepared by the procedure described in [1] were tested in the reaction of carbon dioxide conversion of methane.

TPR was carried out in a flow of the 6%H_2 + Ar mixture at a flow rate of 100 cm^3/min using a thermal-conductivity detector. Heating was carried out at a rate of 12°C/min in the range 20–500°C. Water formed by the reduction was trapped by anhydrone.

Before experiments, all samples were calcined in a flow of dry air at 500°C for 1 h. Air was used to remove water and possible organic impurities from the samples. Preliminary treatment of samples was carried out in the same reactor in a way it was done before TPR runs. To switch the flows, a six-way valve was used.

The amount of consumed hydrogen was determined from the area of the TPR peak with an accuracy of about ±10%. The error in the determination of T_{max} was ±5°C. The final temperature in TPR was somewhat higher than 500°C; this was determined by the capabilities of the temperature controller used in this work. We used in the study the samples calcined at 800°C and samples reduced in a flow of H_2 at 800°C for 40 min. The chosen temperature of calcination corresponded to the temperature of catalytic reaction [1]. The reactor was loaded with a 0.3-g sample.

TPD of O_2 and its adsorption (oxidation) on reduced catalysts was studied on the setup, which involved a DSC-111 (Setaram) differential scanning calorimeter and a system for chromatographic analysis of gaseous reactants and products. In the same setup, we measured the heats of catalyst reoxidation. Details of the procedure were described in [11]. To study oxygen adsorption, the cell of a calorimeter was charged with a sample (0.15 g), heated in a flow of air to 700°C and kept at this temperature for 30 min. Then, it was cooled in a flow of air to 50°C, which was replaced by a helium flow. The latter was used to remove excess oxygen from the reactor. Then, the sample was heated again in a flow of helium at a rate of 10°C/min to 710°C while withdrawing gas samples for analyses every 4 min. The chromatographic setup enabled the separation and detection of H_2, O_2, N_2, CO, CO_2, CH_4, and other gases. During TPD, only O_2 was evolved. Nitrogen adsorption and desorption was not observed. Therefore, air could be used as a source of O_2 in the oxidation of samples.

To determine the extent of reduction, a 0.15-g sample was charged into the calorimeter cell, heated to 700°C in a flow of air, kept at this temperature for 30 min, and successively replaced the flow of air by helium (30 min), 10%H_2–He (30 min), and helium again. Then, a series of air pulses were introduced at 7-min intervals into the helium flow. The conversion of oxygen and the evolution of heat were measured.

The distribution of active elements in initial and reduced samples was studied by LXSA and SEM using a Cameca MBX-1M scanning X-ray micro analyzer. Scanning by an electron probe enabled us to enlarge the image of the sample surface. With this goal, we used secondary and reflected electrons and characteristic X-rays. The images thus obtained provided information on the quantities of phase components and their distribution over the sample bulk.

Before the LXSA study of the sample, the whole amount of the catalyst was ground in a mortar and formed as a single pellet (1–4 g). Then, part of the pellet was ground and fractionated. The 0.25–0.50 mesh fraction (50 mg) was used in the catalytic tests. The rest of the pellet was divided into portions, 10–20 mg each, and used for quantitative analyses and TPR. Thus, all experiments were performed using the same big pellet. LXSA data refer to the distribution of Ni and Cr over the 20-μm subsurface layer (as in any X-ray fluorescence analysis). The complete picture of distribution can be obtained by scanning the sample surface if the trajectories of scanning are close to each other (small-step scanning). For the quantitative analysis of the catalyst components, the absolute value of the intensity of a signal obtained from the test sample was compared with the signal from a standard, which was mounted on a holder in a spectrometer next to the sample. The analyses were accurate to 5–10%.

SEM enabled us to draw conclusions on the composition of the sample surface, because the areas enriched in any element (areas with different phase compositions) may have different contrasts. The X-ray fluorescent analysis of these areas made it possible to check observations in the SEM mode, because the contrasts are sometimes due to morphological features of a particle rather than to the phase composition.

The specific surface area of the test samples was between 17 and 42 m^2/g (see [1]), and the dispersity was $(4–9) \times 10^{-6}$ cm (the size of primary particles)

RESULTS

Temperature-programmed reduction. The method of temperature-programmed reduction was used to study the forms of Ni in the catalysts. We assumed that the reduction of Ni at 800°C occurs not only in the phase of nickel oxide, but in the solid solution $Ni_xMg_{1-x}O$ as well (nickel that strongly interacts with the support). The oxidation of reduced sample should result in the formation of a separate phase of nickel oxide in a greater amount than in the initial sample (before reduction at 800°C).

TPR spectra of the catalysts are shown in Fig. 1 and Table 1. In the spectra of a NiO/MgO catalyst that contained 5% NiO without additives, there is a broad nonintense peak with T_{max} at 190–260°C and a rapid growth of H_2 consumption is observed near 500°C. The

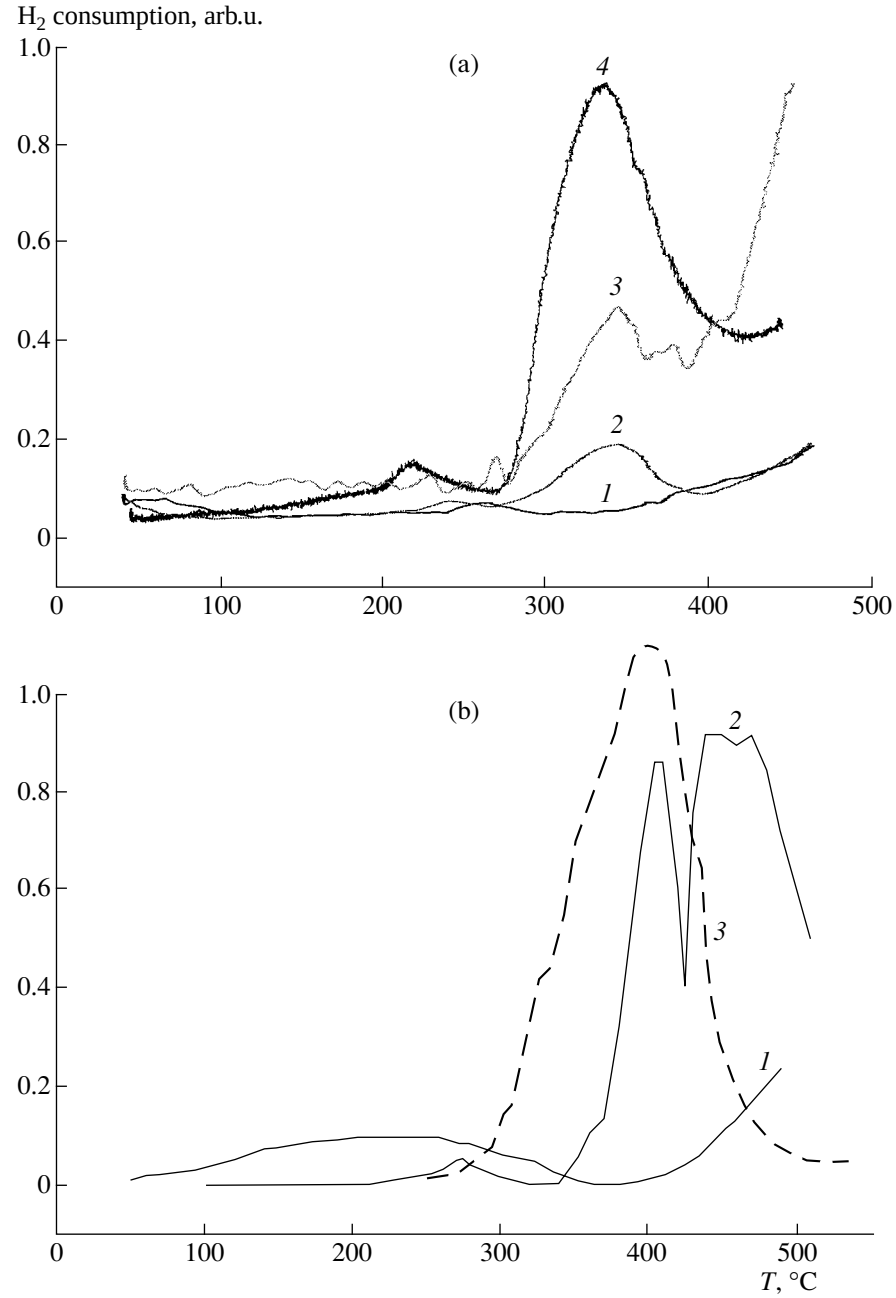

Fig. 1. Temperature-programmed reduction of the catalyst at 20–500°C: (a) samples: (*1*) 3%NiO/MgO, (2) 3%NiO–0.25%Cr_2O_3/MgO (initial), (*3*) 5%NiO/MgO (reduced), and (*4*) 3%NiO–0.25%Cr_2O_3/MgO (reduced); (b) samples: (*1*) 5%NiO/MgO (initial), (*2*) mechanochemically activated 3%NiO/MgO, and (*3*) mechanical mixture 3%NiO + MgO.

second peak apparently continues at temperatures that are much higher than 500°C (Fig. 1b, spectrum *1*).

The TPR spectra of other samples usually have other peaks. An exception is the spectrum of the 6%NiO–2%Cr_2O_3–2%CeO_2/MgO sample, which virtually lacks the low-temperature peak. Thus, when copper oxide is added to the NiO–CeO_2/MgO system, a new peak with T_{max} = 270°C appears in the spectrum, which is characteristic of supported copper reduction $Cu^{2+} \longrightarrow Cu^0$ [12]. However, the extent of copper reduction is low at the same time (23%). The main part of copper oxide probably interacts with support more strongly and is reduced at higher temperatures. In the TPR spectra of samples containing chromium oxide, a maximum appears in the range 380–450°C, and the addition of CeO_2 virtually does not change the TPR picture. Note that the extents of reduction listed in Table 1 (as well as in Table 2) are based on Ni. In fact, we will show below that Cr and other elements also participate in redox processes.

Table 1. Some characteristics of TPR spectra of the catalyst for CO_2 reforming of methane studied in [1]

Sample composition*	T_{max}, °C	H_2 consumption		Ni reduction extent**, %
		mmol/(g Cat)	mol/(g-atom Ni)	
3% NiO/MgO	240	0.002	0.005	0.3
5% NiO/MgO (in)	190–260	0.035	0.05	5.2
5% NiO/MgO (red)	380	0.05	0.03	7.5
6% NiO/MgO (in)	285	0.03	0.04	3.3
6% NiO/MgO (red)	380–500 (steps)	0.026	0.3	32.5
3% NiO–0.25% Cr_2O_3/MgO (in)	380	0.034	0.09	8.5 (2.1)
3% NiO–0.25% Cr_2O_3/MgO (red)	240	0.016	0.04	4.0 (1.0)
	380	0.35	0.9	87.5 (21.9)
6% NiO–2% Cr_2O_3/MgO	150–200	0.04	0.05	5.0 (1.3)
	450	0.19	0.23	22.6
1.5% Cr_2O_3/MgO	470	0.11	–	(18.8)
5% NiO–2% CeO_2/MgO	170–200	0.04	0.06	6.0
6% NiO–2% Cr_2O_3–	(150)	0.002	0.003	0.35
–2% CeO_2/MgO	440	0.20	–	–
5% NiO–2% CuO–	180	0.015	0.02	2.2
–2% CeO_2/MgO	270	0.058	–	–
3% NiO/MgO***	280	0.0036	0.01	0.9
	400	0.053	0.14	13.3
	430–480	0.12	0.31	30.0
3% NiO + MgO (mechanical mixture)	400	0.36	0.9	90
MgO	360	0.01	–	–
Cr_2O_3	370–380	0.03	–	–

* Weight percents correspond to the number of metal gram-atoms per a gram of sample. The oxidation state of chromium in the 3%NiO–0.25%Cr_2O_3/MgO catalyst is not known exactly, and formula Cr_2O_3 is conditional; "in" refers to an initial sample; "red" refers to a reduced sample.

** The extent of chromium reduction is given in parentheses.

*** The sample was obtained by mechanochemical treatment.

It is known that the temperature of supported oxide reduction is in many cases higher than that of the bulk oxide and depends on the strength of metal–support interaction. Thus, the reduction of nickel in the NiO/SiO_2 system occurs at 400–500°C [13–15] although bulk nickel oxide is reduced at ~350°C. Therefore, we conclude that the main portion of nickel in all initial samples is at the state of strong interaction with MgO, probably in the form of the solid surface solution $Ni_xMg_{1-x}O$ formed after the high-temperature treatment during catalyst preparation.

A broad low-temperature peak (150–260°C) in TPR spectra of the NiO/MgO samples can be associated with the existence of a small amount of finely dispersed bulk NiO, which is not bound to the support, or with a small amount of Ni_2O_3 formed after calcination at 800°C. As can be seen from Table 1, in the TPR spectra of preliminarily reduced samples containing 5 and 6%NiO have maxima at 380 and 380–500°C.

The TPR spectrum of the mechanical mixture 3%NiO + MgO differs from both the spectrum of the supported 3%NiO/MgO catalyst and the spectrum of mechanically activated 3%NiO + MgO sample. The spectrum of the mechanical mixture shows only one peak at 400°C, which corresponds to the maximal extent of reduction (90%). This peak is absent from the spectra for the other catalysts and can reasonably be assigned to the reduction of the NiO phase to Ni. The spectrum of the mechanically activated 3%NiO + MgO sample contains three peaks and the overall extent of reduction is lower.

Note that MgO used in this work contains the admixtures of CaO and transition metal oxides (1–2%). According to XRD data, the CaO admixture reacts with CrO_3 in the initial Ni–Cr–O_x/MgO sample and forms chromate $CaCrO_4$ (~1%). Some small amount of H_2 can be consumed for the decomposition (or reduction) of transition metal oxide admixtures (the maximum at 360°C, see Table 1). However, the intensity of the peak with T_{max} = 360°C in the spectrum of MgO is too low to allow the process on the support surface to account for

the presence of intense maxima of H_2 consumption in the presence of Ni and Cr.

The results of the study of the dependence of H_2 consumption maximum and the amount of consumed H_2 on the concentration NiO at the constant concentration of Cr_2O_3 (2%) and on the concentration of Cr_2O_3 at the constant concentration of NiO (3%) are summarized in Table 2 and Fig. 2a. Figure 2b shows the dependence of the extent of reduction on the [Ni]/[Cr] ratio.

As can be seen from these data, if [Ni] < [Cr] (samples with a NiO concentration below 2%), the extent of nickel reduction is high. In this case, the temperature of catalyst reduction (465°C) is close to T_{max} in the spectrum of the CrO_x/MgO sample without nickel (470°C). Obviously, in this case the $MgCrO_4$ chromate is reduced to $MgCr_2O_4$, $NiCrO_4$ is reduced to $Ni_2Cr_2O_4$, and the $CaCrO_4$ admixture is reduced to $CaCr_2O_4$. With an increase in the concentration of Cr_2O_3, the extent of nickel reduction reaches the maximum corresponding to the $NiCr_2O_4$ phase. If the molar concentration of NiO is higher than the concentration of Cr_2O_3, then the extent of reduction substantially decreases (Table 2), and T_{max} approaches the corresponding value for the NiO/MgO samples. With an increase in the NiO concentration at a constant concentration of Cr_2O_3 of 2% (Fig. 2a), the extent of nickel reduction decreases.

The initial portion of the plot of the extent of nickel reduction vs. [Ni]/[Cr] (Fig. 2b) can be associated with the participation of the admixture $CaCrO_4$ phase in reduction. At [Ni] ≈ [Cr], the extent of reduction passes through a maximum. A further increase in the [Ni]/[Cr] ratio is accompanied by a linear decrease in the extent of Ni reduction. This can be explained by the dilution of the $NiCrO_4$ phase by the $Ni_xMg_{1-x}O$ phase.

An increase in the concentration of NiO at a constant Cr_2O_3 concentration results in a decrease in the T_{max}, and an increase in the concentration of Cr_2O_3 at a constant NiO results in a small increase in T_{max}.

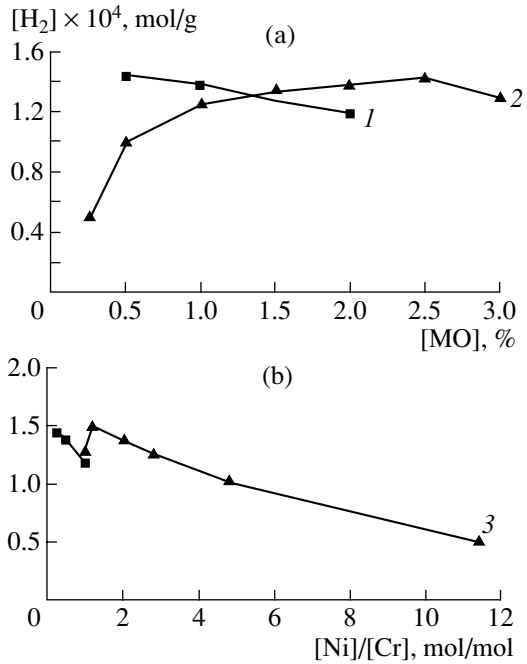

Fig. 2. Dependence of the amount of H_2 consumed by the reduction of the Ni–Cr–O_x/MgO catalyst (*1*) on the concentration of NiO at a constant concentration of Cr_2O_3 equal to 2%, (*2*) on the concentration of Cr_2O_3 at a constant concentration of NiO equal to 3%, and (*3*) on the molar [Ni]/[Cr] ratio.

Thermal desorption of oxygen. Thermal desorption of oxygen (as well as the reoxidation of reduced samples) can serve to estimate the extents of Ni and Cr reduction after the reductive treatment of a catalyst by

Table 2. The effect of Ni and Cr concentration on the characteristics of TPR spectra

[NiO], %	[Cr_2O_3], %	[Ni] × 10^4, mol/g	[Cr] × 10^4, mol/g	T_{max}, °C	[H_2] × 10^4, mol/g	Extent of Ni** reduction, %
0	1.5	0	3.9	470	1.10	–
0.5	2.0	0.7	5.3	465	1.40	100
1.0	2.0	1.4	5.3	465	1.37	100
2.0	2.0	2.8	5.3	465	1.18	42.0
6.0	2.0	8.4	5.3	450	1.90	22.6
3.0	0.25	4.0	0.7	380	0.34	8.5
3.0	0.5	4.0	1.3	400, 420	1.02	25.5
3.0	1.0	4.0	2.6	400, 420, 440	1.25	31.3
3.0	1.5	4.0	3.9	420, 440	1.33	33.3
3.0	2.5	4.0	6.6	410, 420, 440	1.49	37.3
3.0	3.0	4.0	7.9	420, 440	1.28	32.0

* The overall amount of H_2 calculate over all peaks.
** In percents with respect to supported nickel.

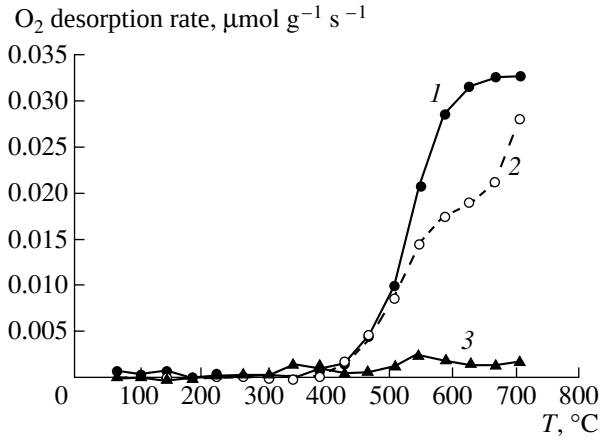

Fig. 3. Thermal desorption of O_2 after its adsorption at 50°C on the catalysts: (*1*) 1.5%Cr_2O_3/MgO, (*2*) 3%NiO–1.5%Cr_2O_3/MgO, and (*3*) 3%NiO/MgO.

hydrogen. Moreover, comparison of the TPD curves for Ni, Cr, and Ni–Cr samples enables the estimation of the efficiency with which Ni and Cr interact in the initial sample.

Figure 3 and Table 3 show the results obtained in the TPD study of oxygen after the preliminary treatment of reduced catalysts by oxygen and sample reoxidation. Before the experiments on O_2 thermal desorption, all samples were treated similarly. In the experiments on the reoxidation of reduced samples, oxidation was carried out at different temperatures to determine the optimal conditions for experimentation.

As follows from the data, the general trends in O_2 adsorption and desorption on Ni/MgO generally corresponds to the picture of NiO/MgO reduction (Table 1). The ratio between the amounts of hydrogen involved in the reduction of various oxide catalysts (Tables 1 and 2) is approximately the same as the ratio between the amounts of oxygen involved in the reoxidation of the corresponding reduced samples (Table 3). The TPD curve of the 3%Ni/MgO sample has two peaks of O_2 evolution, which correspond to weakly and strongly bound oxygen. The amount of oxygen consumed by reoxidation corresponds to the extent of nickel oxide reduction and constitutes several percent of the overall Ni amount. The amount of adsorbed oxygen increases in proportion to the concentration of NI. At the same time, the extent of reduction of NIO increases more rapidly than in proportion with an increase in the concentration of Ni from 3 to 6%. This points to the fact that the extent of nickel reduction in the samples with low NiO concentrations is lower than in the samples with a higher concentration of NiO.

The extent of reduction of the samples containing Cr, including the samples that also contain Ni (in TPR experiments), and the amount of adsorbed O_2 (in the experiments on O_2 thermal desorption) are much greater (more than by an order of magnitude) than the respective characteristics of the NiO/MgO samples. Therefore, we can conclude that supported chromium participates in the redox process. On the O_2 thermal desorption curve for the Cr_2O_3/MgO sample, there is a rapid ascent at ~500°C. On the curve for the NiO–Cr_2O_3/MgO catalyst, there are two jumps (Fig. 3), one of which corresponds to desorption from $CrO_{1.5}$/MgO and the other probably corresponds to the evolution of oxygen from the mixed Ni–Cr phase.

Local X-ray spectral analysis and scanning electron microscopy. The studies using the LXSA and SEM methods were carried out using fresh samples and samples treated in a flow of hydrogen at 800°C. As can be seen from Fig. 4, the uniform distribution of Ni is characteristic of the supported 3%NiO/MgO sample before and after reductive treatment. The average concentration of Ni is 1–1.5% in the initial sample and 2–3% in the reduced sample. Thus, before reduction, the concentration of Ni in the subsurface layer is lower than in the bulk. After reduction, the distributions of Ni are close.

With an increase in the concentration of NiO in MgO to 5–6% (Fig. 5), the uniformity of distribution is disturbed: the islands of the active phase are formed. The concentration of Ni in these islands reaches

Table 3. Thermal desorption of oxygen after the preliminary adsorption of O_2; reoxidation of reduced catalysts supported on MgO

Catalyst		O_2 amount removed during TPD, μmol/g	Heat of reoxidation of the reduced sample*, kJ/mol O_2	Amount of O_2 consumed in reoxidation**, μmol/g			
composition	NiO concentration, μmol/g			H_2: 700°C 30 min O_2: 600°C	H_2: 700°C 30 min O_2: 500°C	H_2: 700°C 30 min O_2: 20°C	H_2: 700°C 30 min O_2: 400°C
3%NiO	402	3.3	305	–	8.7	1.7	–
6%NiO	303	7.0	340	–	28.2	6.4	–
1.5%Cr_2O_3	–	5.4	120–140	–	23.8	16.6	28.7
3%NiO–3%Cr_2O_3	402	43	140–160	314	–	16.2	–

* On the sample containing 1.5% Cr_2O_3 at 600°C; for other samples, at 500°C.
**Conditions of preliminary treatment with hydrogen and the reoxidation temperature are indicated.

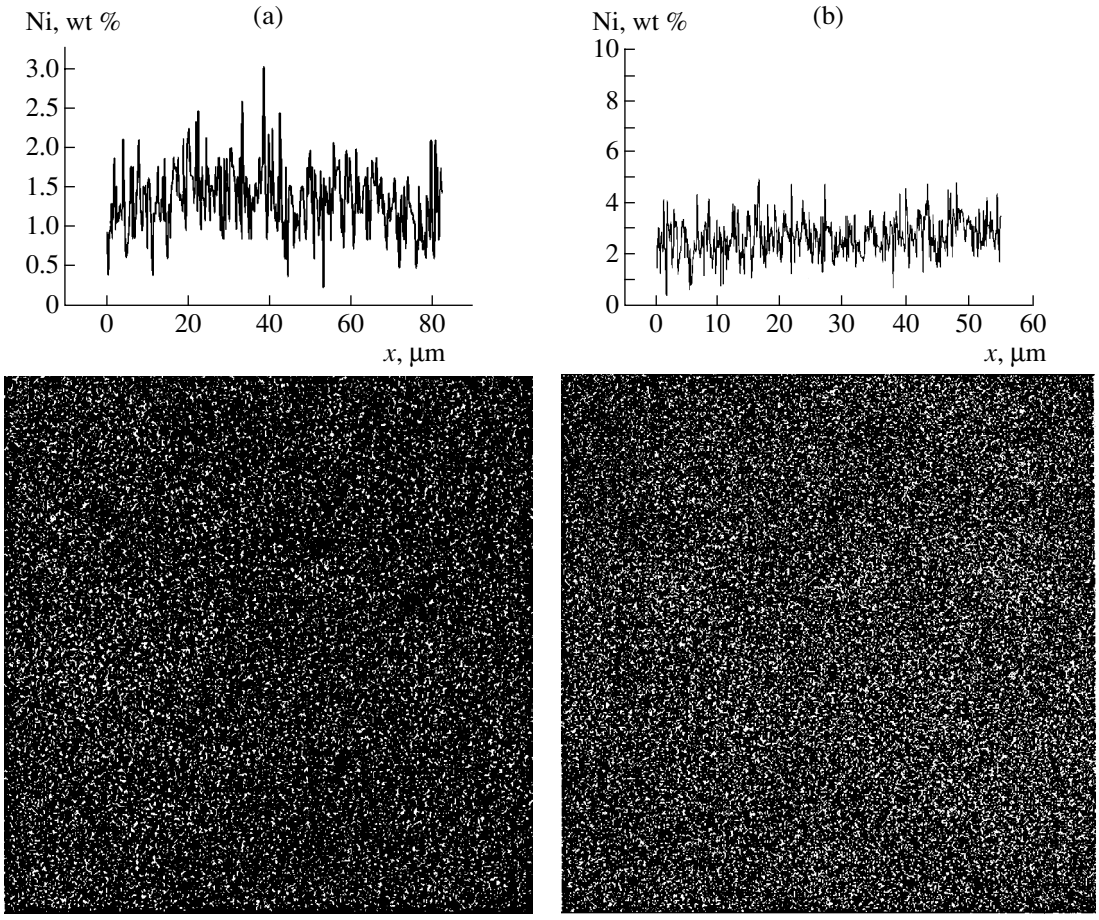

Fig. 4. Local X-ray spectrum of the 3%NiO/MgO catalyst: (a) before reduction and (b) after reduction. On the bottom: X-ray diffraction pattern of a 55 × 55 μm fragment. On the top: the distribution of nickel concentration over the middle line of the bottom figures.

15–25%, whereas the background concentration is 4 wt %, which is close to the average concentration in the sample. The size of islands is 10–20 μm according to XRD and SEM data. After reduction, the number of islands with an elevated concentration of NI increases, but the sizes decrease to 5–10 μm.

The addition of 0.25 wt % Cr_2O_3 into the 3%NiO/MgO sample disturbs the uniform distribution of Ni. As follows from Fig. 6, in the presence of chromium, which is distributed rather uniformly, islands are formed in the sample. The concentration of nickel in these islands reaches 20 wt %, whereas the background concentration of Ni is ~2%. This is lower than the average concentration of Ni in the sample (3%). According to the XRD and SEM data, the size of islands is ~10 μm. The distance between them is 15–20 μm. The reductive treatment results in enlarging the particles, while the distribution of chromium over the sample remains uniform, but its concentration somewhat increases (0.6% instead 0.4%).

The study of the samples prepared by mechanochemical activation (Fig. 7) showed that Ni is distributed nonuniformly over these samples. The 3%NiO/MgO has regions enriched in Ni up to 35 wt %, while the background concentration is ~2%. The size of these regions ranges from 2 to 10 μm. The reduction of the sample at 800°C results in a partial agglomeration of Ni. As a result, the regions are formed on the surface, 10–15 μm in size. This is seen as contrasts on the secondary-electron microscopic images. The addition of chromium oxide does not change the distribution of NiO.

DISCUSSION

NiO/MgO. As noted in [1], the catalytic systems of three types are the most active in carbon dioxide reforming of methane: NiO/MgO with a concentration of NiO higher than 5%, systems based on NiO–Cr_2O_3/MgO with a lower concentration of NiO, and mechanically activated mixtures of NiO and MgO. The data reported in this work obtained by different physicochemical methods show that these systems have many other common features as well.

Let us first consider the NiO/MgO catalysts obtained by impregnation. XRD and TPR studies

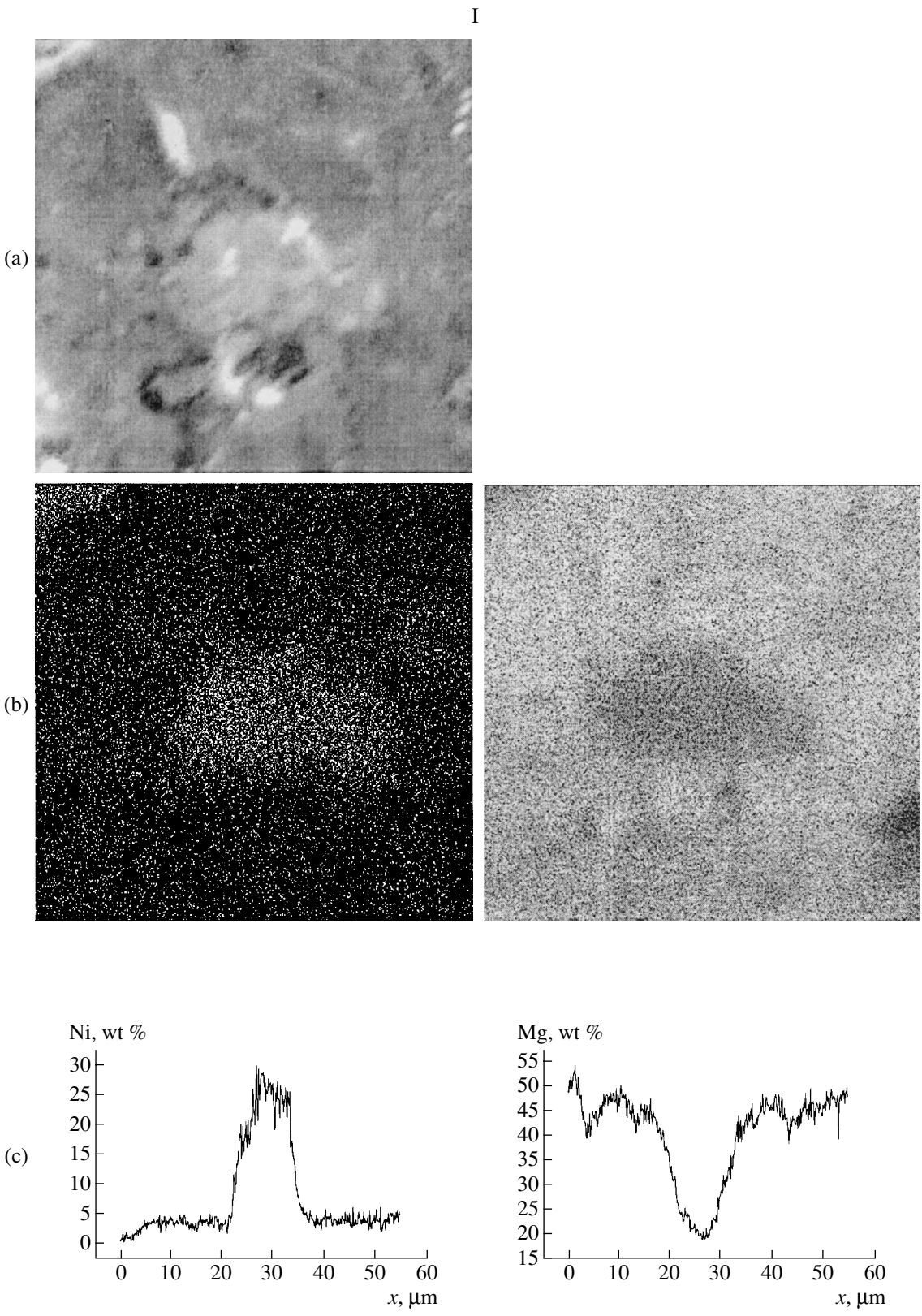

Fig. 5. Local X-ray spectrum and electron microscopic patterns of the 5%NiO/MgO catalyst: (I) Ni and Mg before reduction, (II) Ni after reduction. (a) Scanning electron microscopic patterns of fragments with areas: (I) 55×55, (II, on the left) 110×110, (II, on the right) 55×55 μm fragment; (b) local X-ray spectra for the same fragments; (c) the distribution of nickel and magnesium concentrations over the middle line of the figures.

II

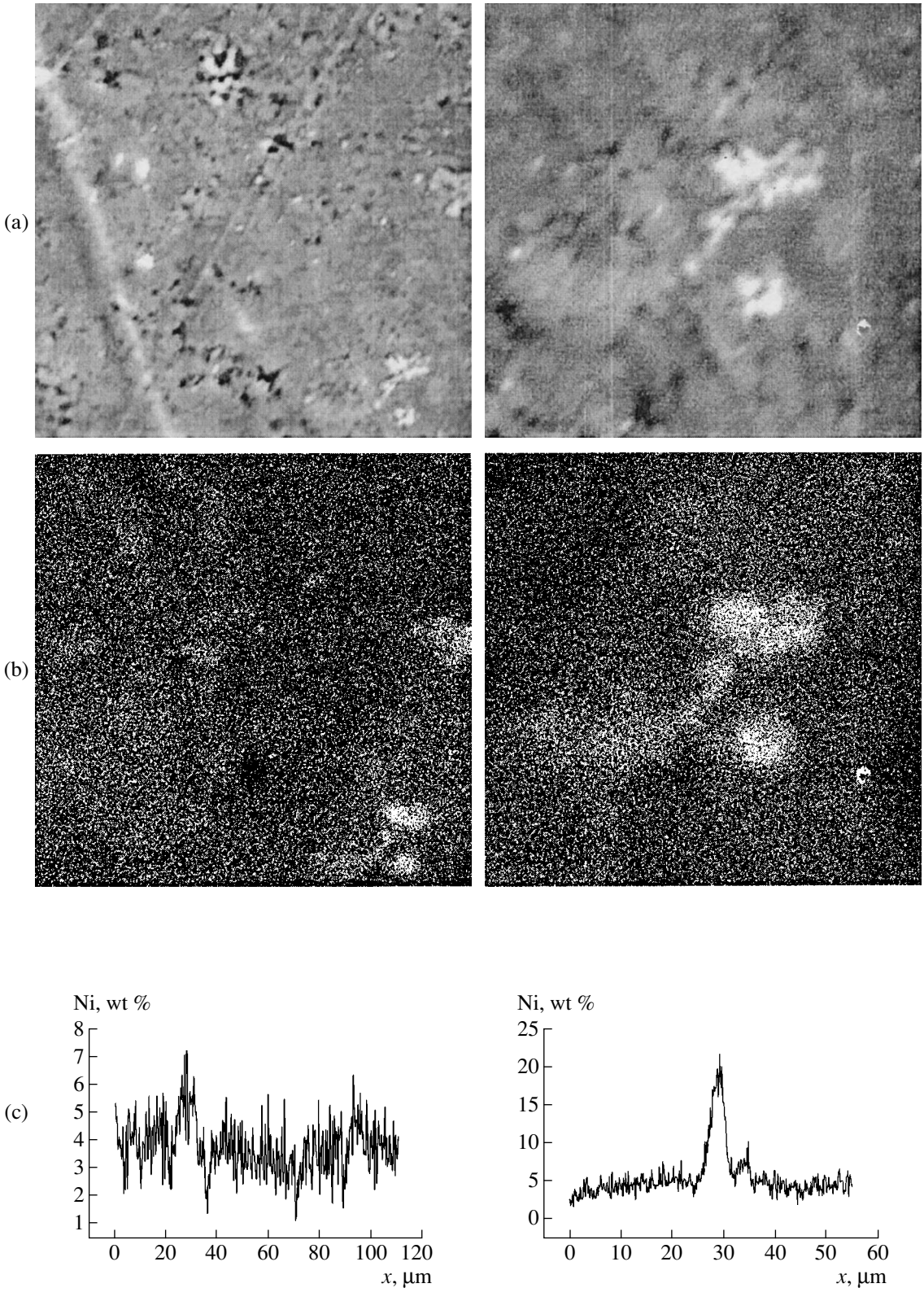

Fig. 5. (Contd.)

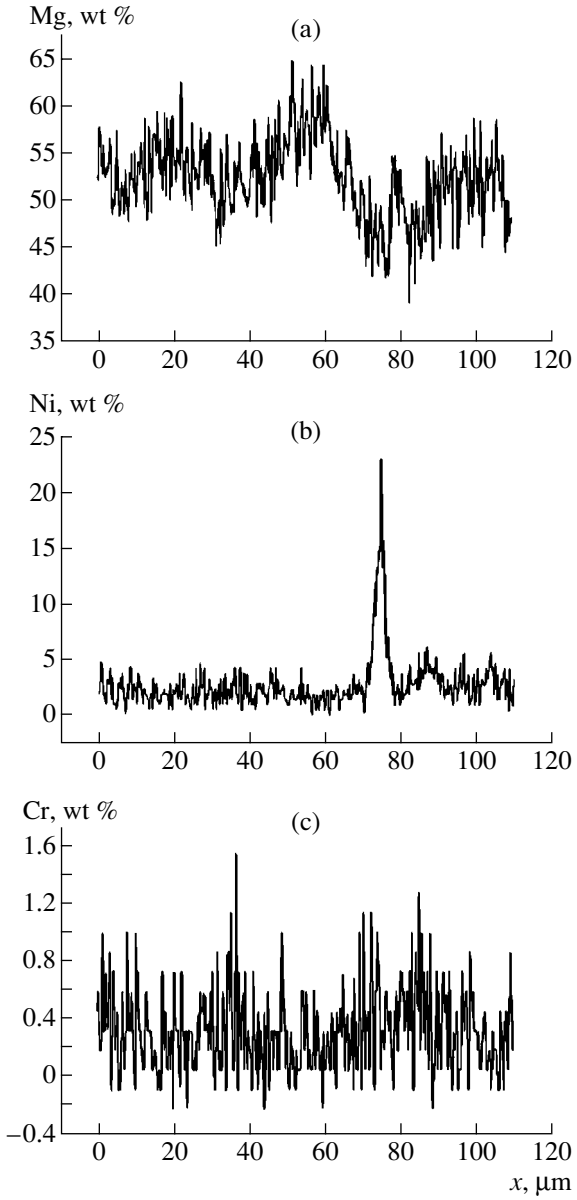

Fig. 6. Distribution of (a) Mg, (b) Ni, and (c) Cr according to LXSA data for the 3%NiO–0.25%Cr_2O_3/MgO catalyst at the 110 × 110 μm fragment before reduction.

showed that the main part of Ni in the initial system belongs to the NiO–MgO composition, whose reduction is difficult. TPR spectra (Fig. 1) point to the substantial difference between the samples with NiO concentrations of 3 and 4–6%. In the first case, only a high-temperature peak is observed (>550°C), which probably corresponds to the solid $Ni_xMg_{1-x}O$ solution. Reoxidation data (Fig. 3) point to the fact that only a small portion of Ni is oxidized and reduced. In the second case, the extent of NiO reduction to Ni is disproportionately high. The peak appears at moderate temperatures (380°C), and preliminary heating in a flow of hydrogen leads to an increase in the amount of reduced nickel. We may conjecture that the preliminary treatment with hydrogen at 800°C is favorable for Ni^{2+} reduction from the surface solid solution. During further oxidation by air at 500°C, metallic particles form the phase of supported NiO, whose reduction temperature is lower than the temperature of nickel reduction from the solid solution.

Earlier, we supposed that strongly oxidized forms of nickel (up to Ni_2O_3) are formed in the samples containing small amounts of NiO. This assumption is supported by calorimetric data (see Table 3). The heat of oxidation of NiO/MgO catalysts (305–340 kJ/mol O_2) is much lower than the value ΔH for the reaction $2Ni + O_2 = 2NiO$ (–479.4 kJ/mol O_2 [16]) and is close to ΔH for the reaction $4Ni + 3O_2 = 2Ni_2O_3$ (–324 kJ/mol O_2). With an increase in the concentration of NiO, the heat of Ni oxidation becomes higher. This can be explained by a decrease in the number of nickel–oxygen clusters on the surface.

The difference in the properties of supported 3%NiO/MgO and 6% NiO/MgO catalysts reveals itself when reaction (I) is carried out in the pulse mode. At 700°C, the transformation of reactants into CO and H_2 on the 3%NiO/MgO catalyst is observed only in the first pulse of $CO_2 + CH_4$. Then, this transformation ceases. On the 6%NiO/MgO sample, this "poisoning" is much smaller. The 3% catalyst is reduced much harder than the 6% sample. Therefore, under the conditions of reaction (I), NiO completely transforms into the carbonate and metallic nickel, on which methane dissociates, is not formed.

Data on the extent of Ni oxidation to NiO and on the extent of NiO reduction to Ni (see Tables 1 and 3) point to the high strength of oxygen binding to the metal in the samples where Ni belongs to the solid $Ni_xMg_{1-x}O$ solution. Therefore, when the concentration of NiO is lower than 4% (only solid solution) metallic nickel is not formed upon reduction, and the catalyst is inactive. According to LXSA and SEM data (Fig. 5), at a higher concentration of Ni, islands are formed, which are the clusters enriched in Ni^{2+}. Their reduction leads to the formation of metallic nickel microcrystals, which are responsible for the catalytic activity. These crystals are readily reoxidized.

Thus, there is a correlation between the catalytic activity of the NiO/MgO samples with different NiO-to-MgO ratios and their susceptibility to reduction.

Cr_2O_3/MgO. The TPR spectra of Cr_2O_3/MgO indicate that this catalyst is reduced by hydrogen at a higher temperature than NiO/MgO (470°C). Judging from the amount of hydrogen used (see Table 1), the stoichiometry of reduction is such that the extent of reduction is higher than unity. Data on adsorption and desorption of O_2 on Cr_2O_3/MgO led us to the same conclusion (Fig. 3 and Table 3). We suppose that the oxidation state of chromium changes by three points: $Cr^{3+} \longleftrightarrow Cr^{6+}$.

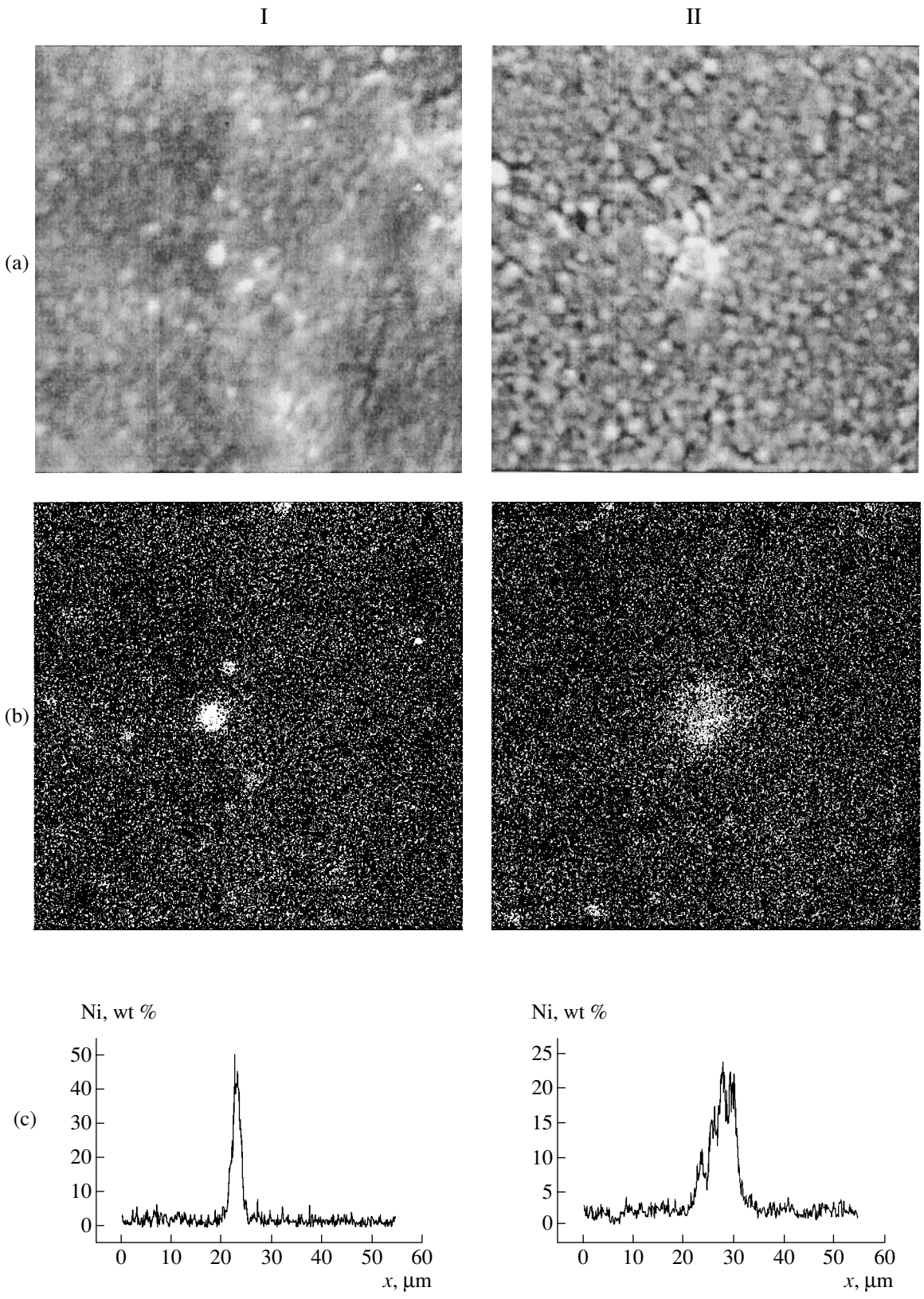

Fig. 7. (a) Scanning electron microscopic patterns of the 55×55 μm fragment, (b) local X-ray spectrum of Ni for the same fragment, and (c) the distribution of the Ni concentration across the middle line of the figure for the mechanically activated 3%NiO + MgO sample: (I) before reduction and (II) after reduction.

The heat of oxidation for the 3%CrO_x/MgO catalyst (120–140 kJ/mol O_2) also points to the possibility of the $Cr^{3+} \longrightarrow Cr^{6+}$ transition, but lower oxidation states are also possible. For the reaction $2Cr_2O_3 + 3O_2 = 4CrO_3$, the value of ΔH is –26.8 kJ/mol O_2. For the reaction $CrO + O_2 = CrO_3$, the value of H_2 is –242.2 kJ/mol O_2 [16].

SEM and LXSA data point to the uniform coverage of the MgO surface by chromium oxide. Chromates and chromites are present on the surface. They can be involved in the following redox transitions:

$$4MgCrO_4 + 6H_2 \longrightarrow 2MgCr_2O_4 + 2MgO + 6H_2O, \quad \text{(IV)}$$

$$2MgCr_2O_4 + 3O_2 + 2MgO \longrightarrow 4MgCrO_4. \quad \text{(V)}$$

Because samples containing MgO also contain CaO, calcium chromate is formed, which is detected by XRD. $CaCrO_4$ is capable of entering redox reactions analogous to reactions (IV) and (V). Note that, according to the literature data [17], the $Ni_{0.03}Mg_{0.97}O$ catalyst is coked less when CaO is added, but the catalytic activity drops. As a result of reduction, the amount of $CaCrO_4$ drastically decreases, and the surface of the CrO_x/MgO catalyst is probably covered by calcium and magnesium chromites.

Ni–Cr_2O_3/MgO. As can be seen from Table 1, in the presence of chromium, the TPR spectra of NiO/MgO samples are characterized by one maximum at 380°C or a broad peak with several maxima at 400–465°C. The temperature ranges of maximal H_2 consumption for the Ni–Cr_2O_3/MgO samples and preliminarily reduced Ni–MgO samples are close. Preliminary reduction in a flow of H_2 at 800°C results in the appearance of the second low-temperature peak with T_{max} = 240°C, and the intensity of the peak with T_{max} = 380°C increases more than 20 times. These extents of reduction have never been observed for the NiO/MgO catalysts without chromium. We suppose that preliminary reduction of chromate to chromite $MgCr_2O_4$ and the formation of isostructural $NiCr_2O_4$ precede the reduction of Ni^{2+} (reaction (IV)). $NiCr_2O_4$ is an intermediate product of the overall reductive process

$$MgCr_2O_4 + NiO \longrightarrow NiCr_2O_4 + MgO, \quad \text{(VI)}$$

$$NiCr_2O_4 + H_2 \longrightarrow Cr_2O_3 + Ni + H_2O. \quad \text{(VII)}$$

Chromium oxide Cr_2O_3 again reacts with MgO:

$$Cr_2O_3 + MgO \longrightarrow MgCr_2O_4. \quad \text{(VIII)}$$

Thus, chromium oxide is the catalyst for NiO reduction to Ni. The probability of reaction $CaCr_2O_4$ with NiO, which is analogous to reaction (VI) is low because $CaCr_2O_4$ and $NiCr_2O_4$ are not isostructural.

During reoxidation by oxygen the reaction

$$2Ni + 2Cr_2O_3 + O_2 \longrightarrow 2NiCr_2O_4 \quad \text{(IX)}$$

can occur or the reaction

$$Ni + MgO + Cr_2O_3 + O_2 \longrightarrow NiO + MgCr_2O_4, \quad \text{(X)}$$

However, ΔH of reaction (X) (–482.7 kJ/mol O_2) is much higher than the experimentally measured oxidation heat (140–160 kJ/mol O_2). This can be explained by the fact that chromium participates in reoxidation or Ni^{3+} (in the highest oxidation state) is formed.

The participation of Cr_2O_3 in the reduction of NiO to Ni is illustrated by curve *2* in Fig. 2. The maximal extent of reduction is achieved at Ni/Cr = 1–2, which is explained by $NiCr_2O_4$ in this process. As the Ni/Cr ratio increases, the extent of reduction decreases almost linearly (Fig. 2b). It is likely that further dilution of the catalyst by nickel oxide does not affect the reduction process. The minimum at the initial portion of the curve in Fig. 2b and the appearance of the maximum can be assigned to the effect of the $CaCrO_4$ admixture. At a high Ni/Cr ratio, excess NiO forms a barely reducible $Ni_xMg_{1-x}O$ oxide, and the amount of consumed H_2 decreases. The amount of H_2 consumed at the point of maximum (1.5×10^{-4} mol/g) is much smaller than the overall amount of NiO (4×10^{-4} mol/g). This means that, another barely reducible nickel compound, e.g. Ni^{2+}, is formed in MgO in addition to $NiCr_2O_4$.

The beginning of the ascent on the thermal desorption curve for Ni–Cr_2O_3/MgO coincides with the ascent on the curve for CrO_x/MgO (Fig. 3). This fact, as well as a large amount of adsorbed oxygen (Table 3), shows that mostly chromium participates in the processes of adsorption and desorption of O_2 (see equation (V)).

LXSA and SEM data point to the uniform distribution of chromium and very nonuniform distribution of nickel (Fig. 6). Chromates and then chromites distributed over the surface of MgO are probably favorable for the decomposition of the solid $Ni_xMg_{1-x}O$ solution, as well as nickel agglomeration and reduction according to reaction (VII). As a result, Ni^{2+} ion clusters and then small crystals of metallic Ni appear at a lower concentration of nickel than in the NiO/MgO system. Their amount on the surface in the Ni–Cr_2O_3/MgO system is larger than in the NiO/MgO system.

Mechanically activated NiO + MgO sample. The TPR spectrum of the mechanically activated NiO + MgO sample has maxima at 280 and 400°C and a broad maximum at 430–480°C, which does not correspond to the maxima for the supported NiO/MgO catalyst and the simple 3%NiO + MgO mixture. The overall extent of reduction of nickel at temperatures up to 500°C is 45%, which is much higher than for the supported sample but much lower than for the 3%NiO + MgO mixture (90%). This means that most of nickel does not enter the composition of the solid solution $Ni_xMg_{1-x}O$. Nickel can probably exist in the active form near the MgO surface, although the NiO phase is not formed according to XRD. The catalytic activity of the mechanically activated NiO + MgO sample is much higher than that of the supported 3%NiO/MgO catalyst,

but it is much lower than the activity of the 3%NiO + MgO mixture.

According to LXSA and SEM data, the picture for the mechanically activated NiO + MgO sample has much more contrasts than in the case of the supported NiO/MgO sample. Upon reduction, the contrast becomes more pronounced (Fig. 7). The regions appear with a nickel concentration of 35% (of the overall number of atoms). This points to the almost complete reduction of NiO. Our data suggest that, in the mechanically activated sample, the reduction occurs at stages, grain by grain of NiO.

In the mechanically activated NiO–Cr_2O_3/MgO sample, a chromium compound is distributed more nonuniformly than nickel oxide. As noted above, chromium is distributed over the surface of a supported catalyst in the form of chromate. During mechanical treatment of the NiO–Cr_2O_3/MgO sample, a mixture of NiO, MgO, Mg, or Ca chromate, and Cr_2O_3 are formed.

On the mechanism of carbon dioxide conversion of methane on Ni/MgO and Ni–Cr_2O_3/MgO. Changes in the catalytic activities of the Ni/MgO and Ni–Cr_2O_3/MgO samples depending on their compositions [1] agree well with the described reduction and adsorption of oxygen on the same catalysts. This fact suggests that carbon dioxide reforming of methane occurs over the catalysts studied in this work via the redox mechanism, which is analogous to the mechanism proposed in [18]. Thus, on NiO/MgO, the following reactions may occur:

$$Ni + CH_4 \longrightarrow NiC + 2H_2, \quad \text{(XI)}$$

$$CO_2 + Ni \longrightarrow NiO + CO, \quad \text{(XII)}$$

$$NiC + NiO \longrightarrow 2Ni + CO. \quad \text{(XIII)}$$

In fact, the process is more complicated. A strong positive effect of MgO, as well as the effect of other basic oxides (CaO or MnO), on the rate of reaction (I) suggests the participation of carbonates in the intermediate steps of this reaction.

ACKNOWLEDGMENTS

We thank the Japanese Energy Program NEDO for financial support.

ACKNOWLEDGMENTS

We thank the Japanese Energy Program NEDO for financial support of this work.

REFERENCES

1. Isaev, O.V., Korchak, V.N., Krylov, O.V., *et al., Kinet. Katal.* (in press).
2. Krylov, O.V., *Ross. Khim. Zh.*, 2000, vol. 44, no. 1, p. 19.
3. Arutyunov, V.S. and Krylov, O.V., *Okislitel'nye prevrashcheniya metana* (Oxidative Conversions of Methane), Moscow: Nauka, 1998.
4. Bradford, M.C.J. and Vannice, M.A., *Cat. Rev.*, 1999, vol. 41, no. 1, p. 1.
5. Tokunaga, O. and Ogasawara, S., *React. Kinet. Catal. Lett.*, 1989, vol. 12, no. 1, p. 69.
6. Gronchi, P., Centola, P., Kaddouri, P., and Del Rosco, R., *Proc. V Int. Natural Gas Conversion Symp.*, Amsterdam: Elsevier, 1998, p. 735.
7. Nam, J.W., Chae, H., Lee, S.H., *et al.*, *Proc. V Intern. Natural Gas Conversion Symp.*, Amsterdam: Elsevier, 1998, p. 843.
8. Suzuki, S., Hayakawa, T., Hamakawa, S., *et al., Proc. V Int. Natural Gas Conversion Symp.*, Amsterdam: Elsevier, 1998, p. 783.
9. Krylov, O.V. and Mamedov, A.Kh., *Usp. Khim.*, 1995, vol. 64, no. 9, p. 935.
10. Ruckenstein, E. and Hu, Y.H., *Catal. Lett.*, 1998, vol. 51, nos. 3–4, p. 181.
11. Bychkov, V.Yu., Sinev, M.Yu., Korchak, V.N., *et al., Kinet. Katal.*, 1989, vol. 30, no. 5, p. 1137.
12. Litvin, E.F., Slinkin, A.A., Arkhipov, P., *et al., Kinet. Katal.*, 1987, vol. 287, no. 1, p. 221.
13. Wang, Q., Yao, J., Rong, J., *et al., Catal. Lett.*, 1990, vol. 4, no. 1, p. 63.
14. Zhang, I., Lin, J., and Chen, Y., *J. Chem. Soc., Faraday Trans.*, 1992, vol. 88, no. 14, p. 2075.
15. Yao, H.C. and Yu Yao, Y.F., *J. Catal.*, 1984, vol. 86, no. 2, p. 254.
16. *Termicheskie konstanty veshchestv* (Thermal Properties of Substances), Moscow: VINITI, 1965–1974, no. 5-VII.
17. Chen, Y.-G., Tomishige, K., and Fujimoto, K., *Appl. Catal. A*, 1997, vol. 163, nos. 1–2, p. 235.
18. Kroll, V.C.H., Swaan, H.M., Lacombe, S., and Mirodatos, C., *J. Catal.*, 1996, vol. 164, no. 2, p. 387.